NeuroImage: Clinical 34 (2022) 103015

Contents lists available at ScienceDirect

NeuroImage: Clinical

journal homepage: www.elsevier.com/locate/ynicl

Medulla oblongata volume as a promising predictor of survival in amyotrophic lateral sclerosis

Giammarco Milella, Alessandro Introna, Alma Ghirelli, Domenico Maria Mezzapesa, Ucci Maria, Eustachio D'Errico, Angela Fraddosio, Isabella Laura Simone *

Neurology Unit, Department of Basic Medical Sciences, Neurosciences and Sense Organs, University of Bari "Aldo Moro", Piazza Giulio Cesare 11, 70100 Bari, Italy

ARTICLE INFO

Keywords:
ALS
MRI
Survival
Brainstem
Medulla oblongata

ABSTRACT

Background: Unconventional magnetic resonance imaging studies of the brainstem have recently acquired a growing interest in amyotrophic lateral sclerosis (ALS) pathology since they provide a unique opportunity to evaluate motor tract degeneration and bulbar lower motor neuron involvement. The aim of this study was to investigate the role of brainstem structures as accurate biomarkers of disease severity and predictors of survival.
Materials and Methods: A total of 60 ALS patients and 30 healthy controls subjects (CS) were recruited in this study. Patients were divided in two subgroups according to the onset of the disease: 42 spinal (S-ALS) and 18 bulbar (B-ALS). All subjects underwent 3D-structural MRI. Brainstem volume both of the entire cohort of ALS patients and S-ALS and B-ALS onset were compared with those of CS. In addition the two ALS subgroups were tested for differences in brainstem volumes.
Volumetric, vertex-wise, and voxel-based approaches were implemented to assess correlations between MR structural features and clinical characteristics expressed as ALSFRS-r and its bulbar (ALSFSR-r-B) and spinal subscores (ALSFSR-r-S). ROC curves were performed to test the accuracy of midbrain, pons, and medulla oblongata volumes able to discriminate patients dichotomized into long and short survivors by using Two-Steps cluster analysis. Univariate and multivariate survival analyses were carried out to test the prognostic role of brainstem structures' volume, trichotomized by applying a k-means clustering algorithm.
Results: Both the entire cohort of ALS patients and B-ALS and S-ALS showed significant lower volumes of both medulla oblongata and pons compared to CS. Furthermore, B-ALS showed a significant lower volume of medulla oblongata, compared to S-ALS. Lower score of ALSFRS-r correlated to atrophy in the anterior compartment of midbrain, pons, and medulla oblongata, as well as in the posterior portion of only this latter region. ALSFSR-r-S positively correlated with shape deformation and density reduction of the anterior portion of the entire brainstem, along the corticospinal tracts. ALSFSR-r-B instead showed a positive correlation with shape deformation of the floor of the fourth ventricle in the medulla oblongata and the crus cerebri in the midbrain. Only medulla oblongata volume demonstrated a significant accuracy to discriminate long and short survivors ALS patients (ROC AUC 0.76, $p < 0.001$). Univariate and multivariate analysis confirmed the survival predictive role of the medulla oblongata (log rank test p: 0.003).
Discussions: Our findings suggest that brainstem volume may reflect the impairment of corticospinal and corticobulbar tracts as well as lower bulbar motor neurons. Furthermore, medulla oblongata could be used as an early predictor of survival in ALS patients.

1. Background

Amyotrophic lateral sclerosis (ALS) is a fatal neurodegenerative disease known for its extremely heterogeneous natural course (Chio et al., 2011). Early identification of patients characterized by a faster disease progression rate is one of the primary goals in the field of motor

Abbreviations: ALS, Amyotrophic lateral sclerosis; B-ALS, bulbar ALS; S-ALS, spinal ALS; CS, control subjects; ALSFSR-r-S, ALSFRS-r spinal subscore; ALSFRS-r-B, ALSFRS-r-bulbar subscore.

* Corresponding author at: Neurology Unit, Department of Basic Medical Sciences, Neurosciences and Sense Organs, University of Bari "Aldo Moro", Piazza Giulio Cesare 11, 70124 Bari, Italy.
E-mail address: isabellalaura.simone@uniba.it (I.L. Simone).

https://doi.org/10.1016/j.nicl.2022.103015
Received 11 October 2021; Received in revised form 29 March 2022; Accepted 19 April 2022
Available online 22 April 2022

neuron diseases. Not only this would allow to timely intervene with therapeutic approaches such as non-invasive ventilation and percutaneous endoscopic gastrostomy (Miller et al., 2009), but also to accurately stratify newly diagnosed patients at the time of enrolment in clinical trials (Hardiman et al., 2011).

Magnetic Resonance Imaging (MRI) has progressively acquired greater relevance to assess *in vivo* the extent of central nervous system damage in ALS patients, given its accessibility and non-invasiveness. Previous unconventional MRI studies unravelled several core imaging features related to the pathogenesis of ALS, including degeneration of the precentral gyrus (Bede et al., 2013; Schuster et al., 2014), corpus callosum (Schuster et al., 2016) and corticospinal tracts (CST) (Ciccarelli et al., 2009). The correlation between atrophy in these structures and disease progression rate (Mezzapesa et al., 2013; Spinelli et al., 2020), King's College staging (Floeter et al., 2018), and disease severity expressed as ALSFRS-r (Grosskreutz et al., 2006) suggested the use of these MRI metrics to evaluate the effect of new therapeutic approaches in ALS (Distaso et al., 2021; Wainger et al., 2021). However, none of them has received a universal consensus, since they seemed not to fully characterize the broad clinical spectrum of ALS disease (Grolez et al., 2016).

A growing interest was recently aroused by radiological studies of the brainstem. This neuroanatomical region potentially gives the opportunity to acquire several information regarding the involvement of both CSTs and motor nuclei of different cranial nerves, respectively. Although brainstem atrophy has always been considered a hallmark of ALS pathology (Clarke and Jackson, 1867), only few MRI studies have been performed to evaluate *in vivo* the involvement of this structure, and, not surprisingly, all of them confirmed degeneration of both white and grey matter in this neuroanatomical region in ALS patients (Bede et al., 2019; Grolez et al., 2018).

Therefore, in the present study we investigate the role of brainstem structures, namely midbrain, pons and medulla oblongata, as accurate biomarkers of disease severity and survival.

2. Materials and methods

2.1. Population

A total of 108 incident ALS patients who referred to our ALS tertiary center between 2018 and 2020 were consecutively recruited at the time of diagnosis. A careful diagnostic work-up was performed to exclude ALS-mimicking diseases. All patients met the criteria for clinically definite (n = 29), probable (n = 44) or possible (n = 35) ALS according to El-Escorial revised criteria (Brooks, 1994). Among these patients, 48 were excluded due to psychiatric illness or use of psychiatric drugs (n = 13), neurological comorbidities (e.g. stroke, trauma) (n = 15), or unable to undergo MRI acquisition due to claustrophobia, presence of metal plaques, or lack of adequate MRI sequences (n = 20). Ultimately, 60 ALS patients with analysable MRI data were included in the study. None of them fulfilled criteria for ALS-Frontotemporal dementia according to Strong criteria (Strong et al., 2017). Genetic analyses for all common ALS related genes were negative in all but one patient, which showed C9orf72 hexanucleotide repeat expansion. Demographic characteristics and clinical data have been registered and collected by experienced neurologists of the ALS team. The following demographic and clinical variables were recorded: age at symptom onset (AAO), gender, onset to diagnosis interval (ODI), age at diagnosis (corresponding to the first neurological clinical evaluation), site of symptom onset, and clinical phenotypes (Chio et al., 2011).

All patients were functionally evaluated using the ALS Functional Rating Scale-Revised (ALSFRS-r), based on 12 items including: bulbar symptoms (1st-3rd items), limb/axial function (4th-9th items) and respiratory symptoms (10th −12th items), each ranging 0–4 (Cedarbaum et al., 1999). For each patient, selective bulbar and spinal subscores of the scale were also calculated (ALSFSR-r-B as the sum of the first three items and ALSFRS-r-S as the sum of the following six items). Longitudinal clinical evaluations were performed at 4–6-months interval and data regarding death or tracheostomy were recorded. Censoring date was set on March 31, 2021. Tracheostomy or death (if occurred) were considered as outcomes.

Control subjects (CS) consisted of 30 subjects not affected by inflammatory, autoimmune, vascular or neurodegenerative diseases, without family history of ALS, and without brain MRI abnormalities.

2.2. MRI acquisitions

All participants underwent MRI on a Philips MRI system 1.5 T scanner. Specifically, ALS patients underwent MRI at time of diagnosis, concurrent with their first neurological evaluation. Routine T1-, T2-weighted and fluid-attenuated inversion recovery (FLAIR) sequences were performed to exclude other causes of focal or diffuse brain damage, including lacunar and extensive cerebrovascular lesions. 3D-structural MRI was acquired using a T1-weighted MP-RAGE (magnetization-prepared rapid acquisition with gradient echo) sequence (TR/TE/flip angle: 25.00 msec/4.60 msec/30.00 degree; Field of View [FOV]: 240 mm; matrix 256x256, voxel size 0.93x0.93x1.0 mm^3).

2.3. MRI analysis

2.3.1. Volumetric analysis

FreeSurfer (version 7.0) image analysis suite (Fischl, 2012) was used for the pre-processing of T1-weighted data: non-brain tissue was removed; subcortical white matter and deep grey matter structures were segmented according to a specific atlas (Grachev et al., 1999). Intensity normalization, tessellation of the grey matter-white matter boundary, and automated topology correction were performed. Subsequently, midbrain, pons, and medulla oblongata volumes were obtained using the Freesurfer's tool "*segmentBS.sh*". Segmentation was conducted using a robust and accurate Bayesian algorithm relying on a probabilistic atlas of the brainstem and neighbouring anatomical structures implemented in Freesurfer (Iglesias et al., 2015). Raw volumetric values were kept for each study participant for further statistical analysis.

Total intracranial volume (TIV) was measured by FMRIB v6.0 Software Library (FSL) in each subject and it was used as a covariate for subsequent analyses. Each subject's brain was skull-stripped and linearly aligned to the standard MNI152 brain image; then, the inverse of the determinant of the affine registration matrix was calculated and multiplied by the size of the template. FSL-FLIRT was used for registration to template (Jenkinson and Smith, 2001), and tissue type segmentation was performed using FSL-FAST (Zhang et al., 2001).

2.3.2. Vertex wise analysis

Shape analysis was performed to characterise anatomical patterns of degenerative changes in the brainstem beyond overall volume reductions,. The FSL tool "*FIRST*" was used for subcortical segmentation of brainstem. During registration, raw 3D T1 images were transformed to Montreal neurological Institute 152 (MNI152) template by standard 12 degrees of freedom and accurately registered to MNI brainstem mask to exclude voxels outside the brainstem region. Afterward, the quantitative scalar values of the brainstem were generated and projected on an average study-specific template (positive value being outside the surface and negative values inside).

2.3.3. Region of interest morphometry

Voxel based morphometry (VBM) was performed using FSL tool "*FSL_VBM*" to detect focal density alterations within the brainstem. After brain extraction and tissue-type segmentation, all subjects' grey-matter partial volume images were aligned to the MNI152 standard space using affine registration. Subsequently, each patient's grey matter images were nonlinearly co-registered to a study specific template.

3. Statistical analysis

ALS demographic and clinical variables were reported as median (along with IQR) or frequencies (percentages) for continuous and categorical variables, respectively. Group differences in the demographic between the entire cohort of ALS patients and CSs were evaluated using a Mann-Whitney *U* test for continuous variables and Chi-square tests for discrete variables. Analyses of covariance (ANCOVA) were performed to evaluate differences in brainstem volumes between the following groups: CS compared firstly to the entire group of ALS patients, then to S-ALS and B-ALS. Lastly, these latter two groups were tested for differences in brainstem volumes. In the analysis, brainstem volumes were included as dependent variables and study groups as an categorical independent variable. TIV, age at the first neurological evaluation and gender were considered as potential confounding factors (Bede et al., 2014) and they were used as covariates. The estimated marginal values of brainstem volumes generated using the residual methods, (Pintzka et al., 2015) were used for subsequent statistical analyses.

Bivariate models were computed using Spearman correlations to assess correlations between estimated values of midbrain, pons and medulla oblongata volume and clinical scales (ALSFRS-r, ALSFRS-r-B, and ALSFRS-r-S).

In order to highlight brainstem shape modification according to disease severity, single linear regression with clinical parameters were performed for the following contrasts: ALSFRS-r, ALSFRS-r-B, ALSFRS-r-S. Age at first neurological evaluation, gender and TIV were used as covariates (Winkler et al., 2014); probability maps were corrected for multiple comparisons using threshold-free cluster enhancement (TFCE), and a statistical threshold of $p < 0.05$ was considered significant.

Afterwards, a voxel-wise generalized linear model and permutation-based non-parametric testing was used to highlight density alterations for correlations with clinical scales using the tool "randomise" of FSL. In order to improve the statistical power of the analysis, we ran "randomise" with 5000 permutations in a smaller mask using labels of the Harvard-Oxford probabilistic structural atlas (Desikan et al., 2006) and labels of the Talairach probabilistic (Lancaster et al., 2000) atlas to generate a merged brainstem mask, which incorporated medulla oblongata, pons and midbrain. Also in VBM analysis, age at first neurological evaluation, gender and TIV were used as covariates (Winkler et al., 2014) and probability maps were corrected for multiple comparisons using TFCE, with a statistical significant threshold of $p < 0.05$.

To evaluate the prognostic role of brainstem structures, patients were dichotomized into long and short survivors using the Two-Steps cluster analysis (Chiu et al., 2001). This latter analysis has been proved to be very informative for clinical practice, since it handled continuous as well categorical variables (Benassi et al. 2020). Thus, we included in the model the categorical variable (reaching or not the endpoint), the continuous variables (time of observation from onset), and we obtained two clusters of patients, namely long and short survivors. ROC curves were performed to test the accuracy of midbrain, pons, and medulla oblongata volumes to discriminate between long and short survivors.

To perform survival analysis, the following continuous variables were split by applying a k-means clustering algorithm (Bradley and Fayyad, 1998) as following: age at symptoms onset and clinical scores (i.e. ALSFSR-r, ALSFSR-r-B and ALSFSR-r-S) were divided into two clusters, while midbrain, pons and medulla oblongata were divided into three clusters. This latter approach has been shown as a valuable approach for classifying datasets with single and multiple iterations (Dubey et al., 2016) and has been used in previous neuroimaging studies in ALS disease (Trojsi et al., 2021).

Kaplan-Meier survival curves were used to illustrate the distribution of survival and log-rank tests were used to test for differences between groups. All variables associated with survival in univariate analysis were used as covariates in a Cox proportional hazard model with a backward stepwise variable selection, in order to identify factors independently associated with survival. Risks were reported as hazard ratios (HRs) along with their 95% CI. A p-value lower than 0.05 was considered for statistical significance. All statistical analyses were performed using SPSS Statistics package (V. 22).

Table 1
Clinical and demographic characteristics of ALS patients.

Age at symptoms onset (years)	
(median; IQR)	60 (52–67)
Cluster I (centroid; n. of patients)	50 years; 26
Cluster II (centroid; n. of patients)	66 years; 34
Sex (Male/Female)	28/32
Male (%)	(47%)
Age at diagnosis (years)	
(median; IQR)	61 (53–68)
Onset to diagnosis interval (months)	
(median; IQR)	10.5 (5.95–16.62)
Site of onset: Bulbar/Spinal (n. of patients)	18/42
Bulbar (%)	(30%)
ALS phenotypes:	
Classic/Bulbar/Flail arm/Flail leg/Pyramidal/Respiratory/ PLMN/PUMN (n. of patients)	50/4/0/0/1/0/ 5/0
Classic (%)	(83%)
ALSFRS-r at diagnosis	
(median; IQR)	41 (33–44)
Cluster I (centroid; n. of patients)	42, 44
Cluster II (centroid; n. of patients)	27, 16
ALSFRS-r-B subscore at diagnosis	
(median; IQR)	11 (9–12)
Cluster I (centroid; n. of patients)	11; 50
Cluster II (centroid; n. of patients)	7; 10
ALSFRS-r-S subscore at diagnosis	
(median; IQR)	19 (12–22)
Cluster I (centroid; n. of patients)	20; 43
Cluster II (centroid; n. of patients)	9; 17
Midbrain volume (mm^3)	
(Estimated marginal mean*)	5649
Cluster I (centroid; n. of patients)	5897 mm^3; 28
Cluster II (centroid; n. of patients)	5526 mm^3; 8
Cluster III (centroid; n. of patients)	5400 mm^3; 24
Pons volume (mm^3)	
(Estimated marginal mean*)	13807
Cluster I (centroid; n. of patients)	14611 mm^3; 20
Cluster II (centroid; n. of patients)	13869 mm^3; 16
Cluster III (centroid; n. of patients)	13097 mm^3; 24
Medulla oblongata volume (mm^3)	
(Estimated marginal mean*)	3418
Cluster I (centroid; n. of patients)	3628 mm^3; 20
Cluster II (centroid; n. of patients)	3401 mm^3; 20
Cluster III (centroid; n. of patients)	3227 mm^3; 20
Tracheostomy, number of patients (yes/no)	24/36
yes (%)	(40.7%)
Death, number of patients (yes/no)	38/22
yes (%)	(63.3%)
Composite outcome, number of patients (yes/no)	47/13
yes (%)	(78.3%)
Survival time from symptoms onset to composite outcome (months) (estimated median; 95% C.I.)	41 (40.12 – 43.7)

Centroid and n. patients were calculated for age at symptoms onset, total ALSFRS-r, bulbar subscores of ALSFRS-r (ALSFRS-r-B), spinal subscores of ALSFRS-r (ALSFRS-r-S) and volume of each brainstem structure.
* Estimated marginal means were calculated using age at first neurological evaluation, gender and total intracranial volume (TIV) as covariates. (Age at first neurological evaluation = 60.44, gender = 1.47, TIV = 1443686.89).
PLMN: pure lower motor neuron phenotype.
PUMN: pure upper motor neuron phenotype.

4. Results

4.1. Clinical and demographic characteristics

Median AAO was 61 years and median ODI was 10.5 months. Spinal

Table 2
Brainstem volumes in control subjects (CS), ALS patients, spinal onset ALS patients (S-ALS), bulbar onset ALS patients (B-ALS).

Structure	Study group	Estimated marginal means * (mm3)	Standard error	p	Post-hoc comparisons
Medulla Oblongata	**CS**	3821	45	$p < 0.001$	ALS vs CS: $p < 0.001$
	ALS	3418	32		S-ALS vs CS: $p < 0.001$
	S-ALS	3452	39		B-ALS vs CS: $p < 0.001$
	B-ALS	3340	59		B-ALS vs S-ALS: $p = 0.029$
Pons	**CS**	14,513	141	$p < 0.001$	ALS vs CS: $p < 0.001$
	ALS	13,807	98		S-ALS vs CS: $p = 0.004$
	S-ALS	13,894	119		B-ALS vs CS: $p < 0.001$
	B-ALS	13,605	182		S-ALS vs B-ALS: p: NS
Midbrain	**CS**	5730	49		
	ALS	5649	35	$p = NS$	
	S-ALS	5676	42		
	B-ALS	5585	64		

*Estimated marginal means and standard error are adjusted for age at first neurological evaluation, gender, and total intracranial volume. (Age at first neurological evaluation = 60.44, gender = 1.47, TIV = 1443686.89).
NS = not significant.

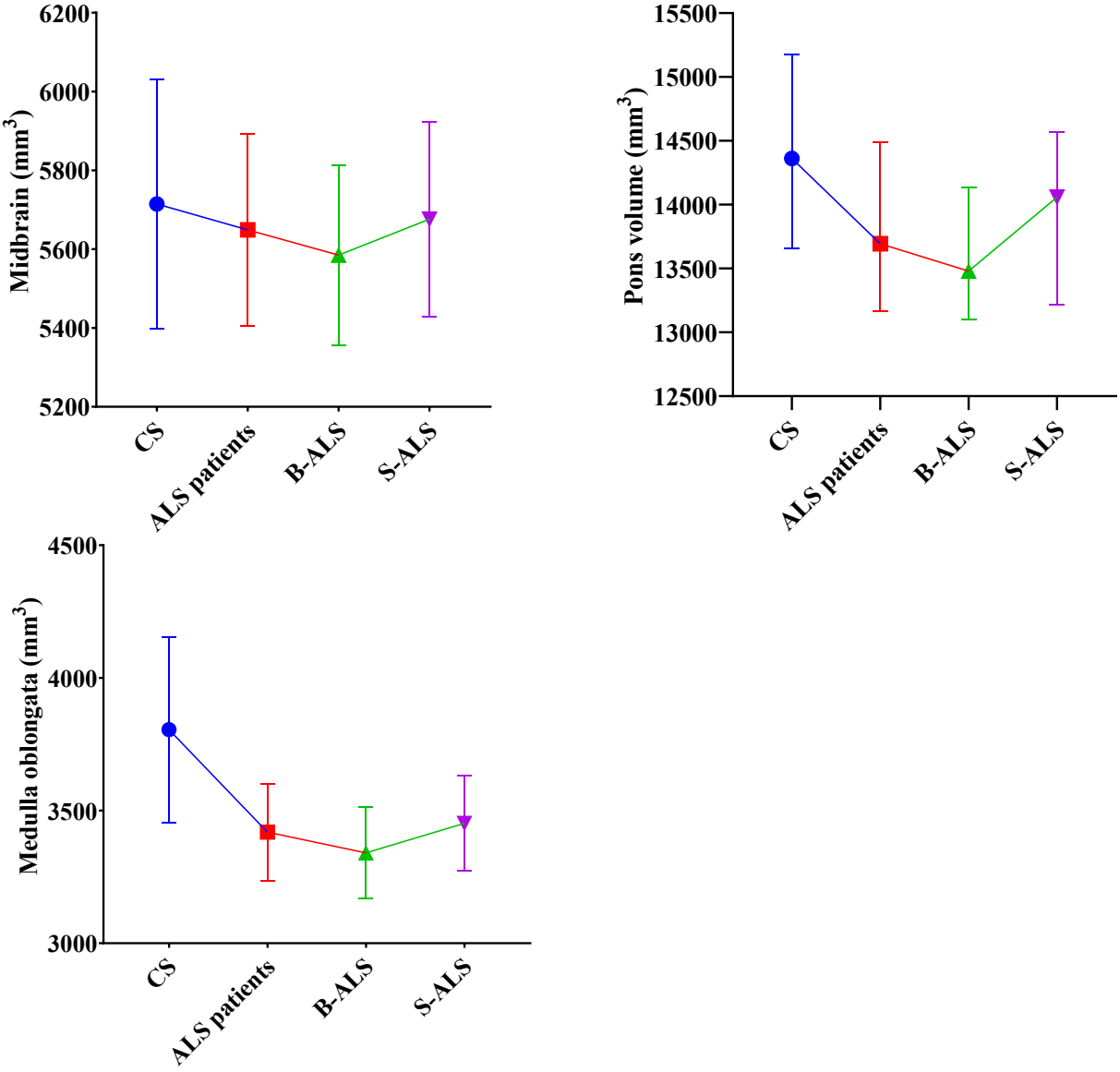

Fig. 1. Estimate marginal means with standard deviations of the midbrain, pons, medulla volumes are plotted for each study group adjusted for age, gender and total intracranial volumes. CS = control subjects B-ALS = bulbar-onset ALS patients S-ALS = spinal-onset ALS patients.

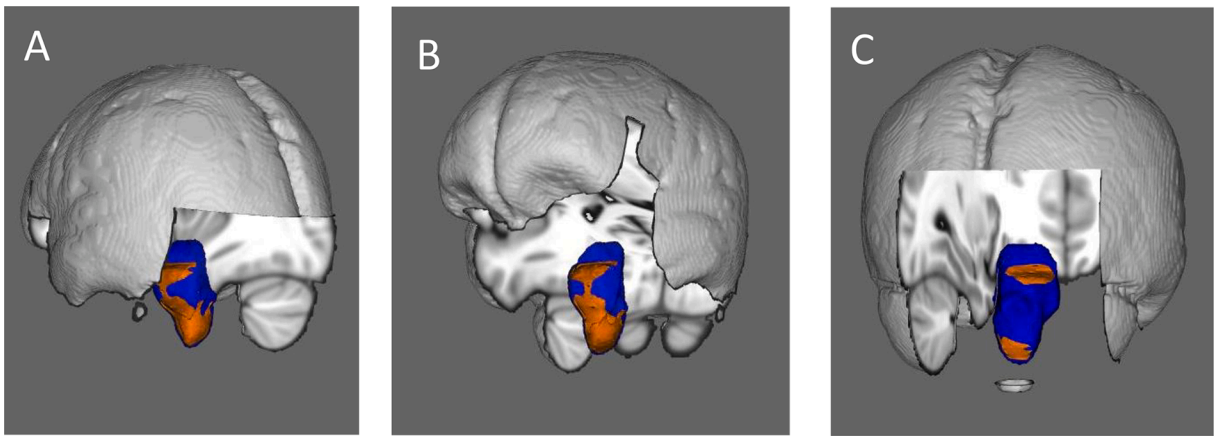

Fig. 2. Anatomical patterns of brainstem pathology based on vertex analyses correcting for age, gender, and total intracranial volumes. Correlations between shape deformation of brainstem and ALSFRS-r score (A), ALSFRS-r-S (B) and ALSFRS-r-B (C) are illustrated in orange. (For interpretation of the references to colour in this figure legend, the reader is referred to the web version of this article.)

onset of disease was more frequent than bulbar onset (70% and 30% respectively). Fifty patients (84%) were classified as classic ALS phenotypes. Median values with relative interquartile range (IQR) and clusters' centroid of age at symptoms onset, total ALSFRS-r, ALSFRS-r-B, ALSFRS-r-S are reported in Table 1. Fifty-one (79%) patients reached the composite outcome (tracheostomy or death) at the censoring date. Estimated median survival time from symptoms onset to combined outcome was 41 months.

CS were sex and age- matched to ALS patients with a median age of 60 years (IQR 53–78) and a male to female ratio of 10/21 (46% male and 54% female).

4.2. Relations between volume of brainstem structures and clinical features

4.2.1. Volumetric MRI analysis

ALS patients showed significant lower volumes of both medulla oblongata and pons compared to CS ($p < 0.001$ for both brainstem structures). Subgroups analysis revealed that ALS patients had lower medulla oblongata and pons volume compared to CS despite the site of onset. Moreover, B-ALS patients were characterized by a wider atrophy of the medulla oblongata, compared to S_ALS patients ($p = 0.029$) (Table 2 and Fig. 1). The only patient tested positive for C9Orf72 hexanucleotide repeat expansion showed values of medulla oblongata, pons and midbrain volume within IQR range of ALS patients (3568 mm^3, 13640 mm^3, 5510 mm^3 respectively).

Midbrain, pons and medulla oblongata volumes positively correlated both with total ALSFSR-r ($r_s = 0.347$, $p = 0.007$; $r_s = 0.369$, $p = 0.004$; $r_s = 0.381$, $p = 0.003$ respectively), ALSFSR-r-S score ($r_s = 0.295$, $p = 0.022$; $r_s = 0.283$, $p = 0.027$; $r_s = 0.284$, $p = 0.028$ respectively). Otherwise, only medulla oblongata volume correlated with ALSFRS-r-B score ($r_s = 0.345$, $p = 0.007$).

4.2.2. Vertex analysis

Vertex analysis confirmed the correlation between total ALSFRS-r score and shape deformation in all brainstem structures, specifically in the anterior compartment of midbrain, pons and medulla oblongata and the posterior portion only of this latter region (Fig. 2a). ALSFRS-r-S score positively correlated with shape deformation of the anterior portion of the entire brainstem, along the corticospinal tracts' course (Fig. 2b). Instead, vertex analysis revealed a significant positive correlation between score of ALSFRS-r-B and shape deformation of the floor of the fourth ventricle in the medulla oblongata and the crus cerebri in the midbrain (where the corticobulbar tracts run) (Fig. 2c).

4.2.3. Brainstem morphometry

VBM analyses implemented the results derived from vertex analyses. Total ALSFRS-r score showed positive correlation with the density of the medulla oblongata *in toto* and the anterior portion of the entire brainstem, confirming that the impairment of these latter *loci* reflects the degree of clinical severity in ALS (Fig. 3a). Furthermore, ALSFRS-r-S score positively correlated with the anterior portion of the brainstem (Fig. 3b), while ALSFRS-r-B score with the posterior portion of the medulla oblongata and crus cerebri (Fig. 3c).

4.3. Relations between volume of brainstem structures and survival

Two-Steps cluster analysis identified two clusters among our cohort study: the first cluster (long survivors) included 13 patients with a mean time of observation of 55 months (standard deviation 13) and none of them reached the composite outcome. The second cluster was composed of 47 patients with a mean time of observation of 35 months (standard deviation 15) and all of them reached the composite outcome. Among all the brainstem structure analysed, only medulla oblongata volume demonstrated a significant accuracy to discriminate the long and short-survivors patients (ROC AUC 0.76 $p < 0.001$) (Fig. 4).

Kaplan-Meier survival curves from symptoms onset failed to detect significant differences between patients grouped according to three cluster volumes of the midbrain and pons, calculated through the k-means clustering algorithm. Only medulla oblongata volume showed a significant impact on survival in the univariate analysis (log-rank $p = 0.003$) (Fig. 5). Furthermore, multivariate analysis showed that medulla oblongata volume was the only independent significant predictor of ALS survival [Hazard Ratio (HR): 2.882; 95% confidence interval (CI): 1.087–7.639; $p = 0.033$, comparing the cluster of patients with greater medulla oblongata volume to those with intermediate medulla oblongata volume; HR: 7.783; 95% CI: 2.015–30.061; $p = 0.003$ comparing the cluster of patients with greater medulla oblongata volume to those with lower volume].

5. Discussion

Our study demonstrated a major brainstem atrophy in ALS patients compared to healthy controls primary driven by reduced volume of pons and medulla oblongata. Furthermore B-ALS patients showed a smaller medulla oblongata volume compared to S-ALS patients. Previous studies highlighted the impairment of these neuroanatomical structures in ALS patients (Bede et al., 2019; Li et al., 2021); innovatively, our data revealed a smaller medulla oblongata volumes in ALS patients with earlier involvement of bulbar district. This latter finding agreed with the

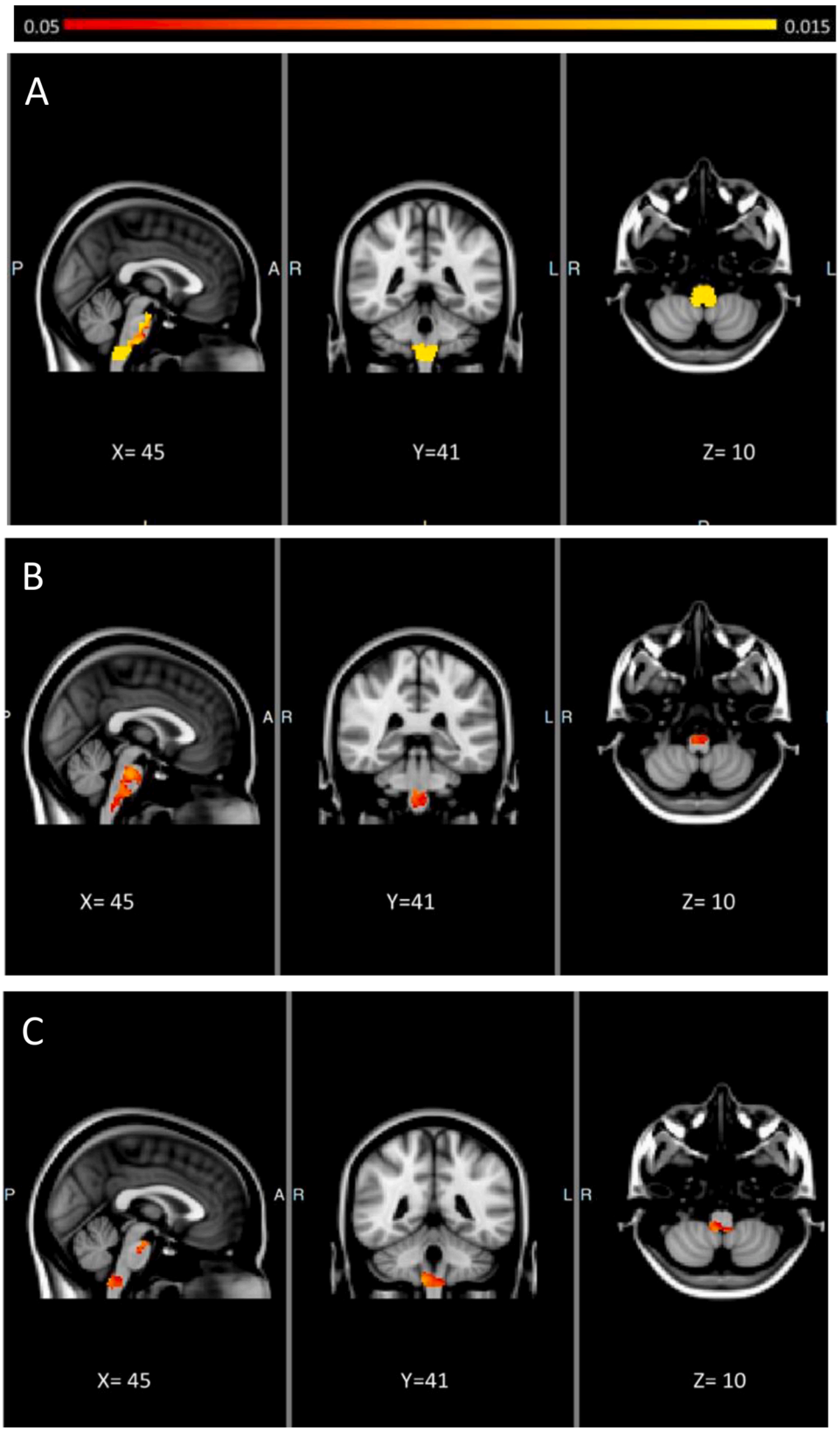

Fig. 3. Morphometric brainstem alterations in ALS patients. Statistical maps are presented in MNI space, MNI coordinates are provided under each view. Morphometric brainstem alterations correlated to ALSFRS-r score (A), ALSFRS-r-S (B), ALSFRS-r-B (C) at $p < 0.05$ TFCE FWE corrected for age, gender and TIV.

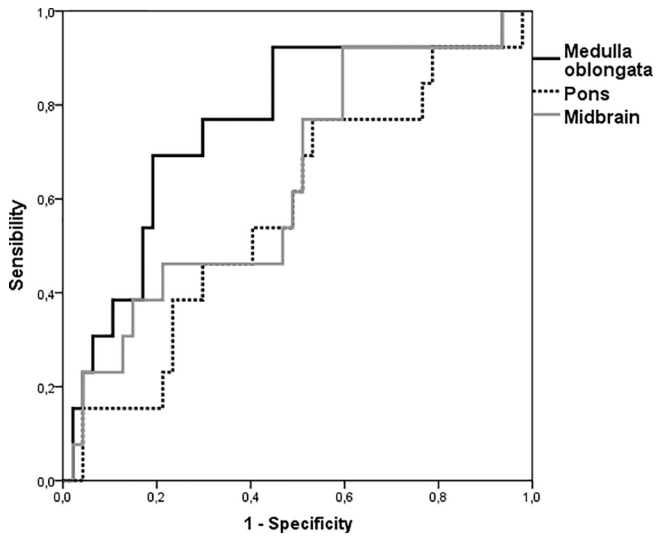

Fig. 4. ROC curves of volumes of midbrain, pons, and medulla oblongata volumes to discriminate long and short survivor ALS patients.

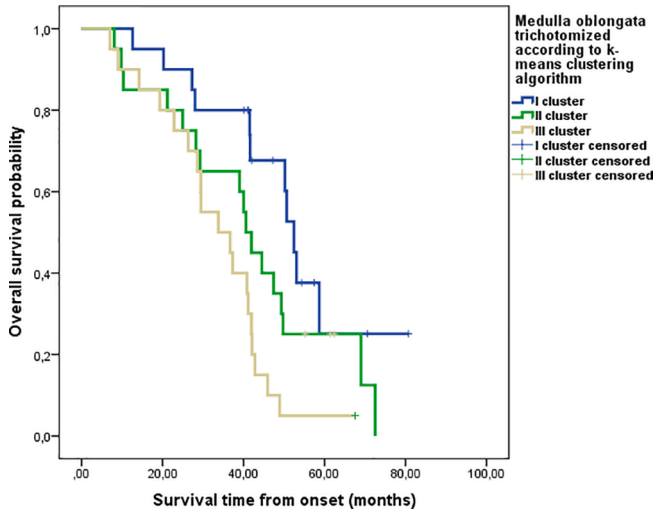

Fig. 5. Kaplan Mayer survival curves in ALS patients stratified according to k-means clustering algorithm of medulla oblongata.

most accredited model of ALS disease spreading, according to which the motor neuron degeneration progresses over time primarily in the neuroanatomical region where hypothetically the disease process began and afterwards in the contiguous regions (Ravits et al., 2007; Ravits and La Spada, 2009).

Furthermore, we verify the role of medulla oblongata, pons, and midbrain volumes as possible biomarkers of disease severity and early predictors of survival in ALS patients.

The strong positive correlation we found between ALSFRS-r score and the volume of these neuroanatomical sites confirms the role of these MRI measures as a global indicator of disease severity. Previous studies have investigated the diagnostic role of brainstem volumes (Bede et al., 2019) unravelling the trajectories of neurodegeneration in this neuroanatomical region over the course of the disease (Bede et al., 2020). Moreover, grey matter loss of the brainstem was found to be associated to pseudobulbar symptoms (e.g. pathological laughter and crying) (Tu et al., 2021). However, to date, only one study has investigated the role of brainstem as a potential indicator of disease severity and the authors reported a significant positive correlation between diffusion tensor imaging (DTI) metrics of several white matter tracts (e.g. fractional anisotropy and radial diffusivity) in these structures and ALSFRS-r score, but not between volumetric measures and this functional clinical scale (Li et al., 2021). Differently from Li et al., our ALS population included almost double participants (60 vs 33), conferring the study a superior statistical sensitivity. Moreover, in the above-mentioned paper, no formal adjustment for age, gender and total intracranial volume was performed before carrying out correlation analyses. Through our work, we reiterate the need to control the volumetric variables for possible confounding factors, as previously reported in literature (Voevodskaya et al., 2014). Additionally, in our opinion volumetric study of the brainstem has several advantages over DTI in common clinical practice. First, 3D T1 sequences can be easily acquired with a good spatial resolution; conversely, DTI sequences require more time to be obtained with possible distortions in the brainstem even after the application of correction measures (Li et al., 2021). Furthermore, voxel-based and shape analysis investigate not only white matter but also grey matter involvement.

As a proof of this latter postulation, using a combination of volumetric, vertex and voxel-based morphometry analyses we demonstrate that brainstem volumes can simultaneously detect the impairment of CSTs, corticobulbar tracts and lower bulbar motor neurons. Several previous studies have shown significant abnormalities of the CST at the brainstem level in ALS patients (Baek et al., 2020; Cardenas-Blanco et al., 2014; Floeter et al., 2014), and most of them agree to consider this neuroanatomical region as a reliable biomarker of UMN impairment. Our study confirms this evidence. To date, only one study found that a lower performance in bulbar functions was associated with lower fractional anisotropy values of the left CST at the brainstem level (Li et al., 2021). Finding radiological biomarkers of selective impairment of corticobulbar tracts originating from upper motor neuron in the cortex could have a great relevance in common clinical practice since it could allow clinicians to reach a higher and earlier level of diagnostic accuracy of ALS, even in absence of clinical evidence.

On the other hand, we demonstrate that the drop of ALSFRS-r bulbar score was due not only to corticobulbar tract impairment but primarily to medulla oblongata atrophy, in particular at the level of the floor of the fourth ventricle, where nuclei of several cranial nerves lie (e.g. IX, X, XII). Although previous MRI studies reported impairment of this neuroanatomical region as a hallmark of ALS disease (Bede et al., 2019), to date our study was the first to propose medulla oblongata volume as a biomarker of selective bulbar LMN impairment.

Considering that impaired bulbar function represents the main source of disability in ALS patients (del Aguila et al., 2003; Stambler et al., 1998) and, either directly or indirectly, it strongly affects survival, it is not surprising that only medulla oblongata volume demonstrated a prognostic role among all brainstem volumes. One could argue that also the midbrain volume should play a prognostic role, since it reflects the damage of UMN tracts running through this neuroanatomical structure. However, it is well known that upper motor neuron burden is better associated with onset and spread of ALS pathology rather than with survival, unlike lower motor neuron impairment (Armon and Moses, 1998). Using a fully automated algorithm and routine MRI sequences we demonstrate that MRI measures are able to predict survival with an accuracy of 80%, in agreement with a previous study of Schuster et al. (Schuster et al., 2017).

Furthermore, in our study, multivariate analysis demonstrates that medulla oblongata volume is the only independent factor associated to death among all demographic and clinical variables commonly associated to survival in literature.

The main limit of our study is the lack of longitudinal MRI analysis that might allow to better define the rate of reduction of medulla oblongata volumes. However, considering the extreme shortness and variability of disease duration in ALS, identifying a second time-point to perform longitudinal MRI acquisition is effortful. Indeed, a previous study failed to detect longitudinal statistically significant changes in brainstem volumes after four months of follow-up (Bede et al., 2019).

Another limit of our study is the lack of a quantitative assessment of pseudobulbar impairment, (e.g. Center for Neurologic Study Lability Scale score (Moore et al., 1997)), and in particular an extensive neuropsychological assessment with standardized screening test (e.g. Edinburgh Cognitive and Behavioural ALS screening (Poletti et al., 2018)).

Notwithstanding these limitations, we demonstrated that brainstem measures derived from T1-weighted data are attractive candidate biomarkers of disease severity and survival in the disease course.

6. Declarations

The authors declare that the present study has been presented as an oral communication to the WCN October 3–7, 2021.

7. Ethics approval

We confirm that we have read the Journal's position on issues involved in ethical publication and affirm that this report is consistent with those guidelines. Ethical approval was waived by the local Ethics Committee considering that all the procedures being performed were part of the routine care.

8. Consent to participate

All patients gave written informed consent to be enrolled in the study.

9. Consent for publication

All patients gave written informed consent to publish data for scientific purpose.

10. Availability of data and material

The data that support the findings of this study are available from the corresponding author, [ILS], upon reasonable request.

Funding

The authors did not receive support from any organization for the submitted work. No funding was received to assist with the preparation of this manuscript. No funding was received for conducting this study. No funds, grants, or other support was received.

Declaration of Competing Interest

The authors declare that they have no known competing financial interests or personal relationships that could have appeared to influence the work reported in this paper.

References

Armon, C., Moses, D., 1998. Linear estimates of rates of disease progression as predictors of survival in patients with ALS entering clinical trials. J. Neurol. Sci. 160 (Suppl 1), S37–S41. https://doi.org/10.1016/s0022-510x(98)00196-8.

Baek, S.-H., Park, J., Kim, Y.H., Seok, H.Y., Oh, K.-W., Kim, H.-J., Kwon, Y.-J., Sim, Y., Tae, W.-S., Kim, S.H., Kim, B.-J., 2020. Usefulness of diffusion tensor imaging findings as biomarkers for amyotrophic lateral sclerosis. Sci. Rep. 10, 5199. https://doi.org/10.1038/s41598-020-62049-0.

Bede, P., Bokde, A., Elamin, M., Byrne, S., McLaughlin, R.L., Jordan, N., Hampel, H., Gallagher, L., Lynch, C., Fagan, A.J., Pender, N., Hardiman, O., 2013. Grey matter correlates of clinical variables in amyotrophic lateral sclerosis (ALS): a neuroimaging study of ALS motor phenotype heterogeneity and cortical focality. J. Neurol. Neurosurg. Psychiatry 84, 766–773. https://doi.org/10.1136/jnnp-2012-302674.

P. Bede, R.H. Chipika, E. Finegan, S. Li Hi Shing, K.M. Chang, M.A. Doherty, J.C. Hengeveld, A. Vajda, S. Hutchinson, C. Donaghy, R.L. McLaughlin, O. Hardiman, 2020. Progressive brainstem pathology in motor neuron diseases: Imaging data from amyotrophic lateral sclerosis and primary lateral sclerosis. Data Brief 29, 105229. https://doi.org/10.1016/j.dib.2020.105229.

P. Bede, R.H. Chipika, E. Finegan, S. Li Hi Shing, M.A. Doherty, J.C. Hengeveld, A. Vajda, S. Hutchinson, C. Donaghy, R.L. McLaughlin, O. Hardiman, 2019, Brainstem pathology in amyotrophic lateral sclerosis and primary lateral sclerosis: A longitudinal neuroimaging study. NeuroImage Clin. 24, 102054. https://doi.org/10.1016/j.nicl.2019.102054.

Bede, P., Elamin, M., Byrne, S., Hardiman, O., 2014. Sexual dimorphism in ALS: exploring gender-specific neuroimaging signatures. Amyotroph. Lateral Scler. Front. Degener. 15, 235–243. https://doi.org/10.3109/21678421.2013.865749.

M. Benassi, S. Garofalo, F. Ambrosini, R.P. Sant'Angelo, R. Raggini, G. De Paoli, C. Ravani, S. Giovagnoli, M. Orsoni, G. Piraccini, 2020, Using two-step cluster analysis and latent class cluster analysis to classify the cognitive heterogeneity of cross-diagnostic psychiatric inpatients. Front. Psychol. 11.

Bradley, P.S., Fayyad, U.M., 1998. Refining initial points for K-means clustering. Morgan Kaufmann 91–99.

Brooks, B.R., 1994. El Escorial World Federation of Neurology criteria for the diagnosis of amyotrophic lateral sclerosis. Subcommittee on Motor Neuron Diseases/Amyotrophic Lateral Sclerosis of the World Federation of Neurology Research Group on Neuromuscular Diseases and the El Escorial "Clinical limits of amyotrophic lateral sclerosis" workshop contributors. J. Neurol. Sci. 124 Suppl, 96–107. https://doi.org/10.1016/0022-510x(94)90191-0.

Cardenas-Blanco, A., Machts, J., Acosta-Cabronero, J., Kaufmann, J., Abdulla, S., Kollewe, K., Petri, S., Heinze, H.-J., Dengler, R., Vielhaber, S., Nestor, P.J., 2014. Central white matter degeneration in bulbar- and limb-onset amyotrophic lateral sclerosis. J. Neurol. 261, 1961–1967. https://doi.org/10.1007/s00415-014-7434-4.

Cedarbaum, J.M., Stambler, N., Malta, E., Fuller, C., Hilt, D., Thurmond, B., Nakanishi, A., 1999. The ALSFRS-R: a revised ALS functional rating scale that incorporates assessments of respiratory function. BDNF ALS Study Group (Phase III). J. Neurol. Sci. 169, 13–21. https://doi.org/10.1016/s0022-510x(99)00210-5.

Chio, A., Calvo, A., Moglia, C., Mazzini, L., Mora, G., 2011. Phenotypic heterogeneity of amyotrophic lateral sclerosis: a population based study. J. Neurol. Neurosurg. Psychiatry 82 (7), 740–746.

Chiu, T., Fang, D., Chen, J., Wang, Y., Jeris, C., 2001. In: A robust and scalable clustering algorithm for mixed type attributes in large database environment, in. Association for Computing Machinery, New York, NY, USA, pp. 263–268. https://doi.org/10.1145/502512.502549.

Ciccarelli, O., Behrens, T.E., Johansen-Berg, H., Talbot, K., Orrell, R.W., Howard, R.S., Nunes, R.G., Miller, D.H., Matthews, P.M., Thompson, A.J., Smith, S.M., 2009. Investigation of white matter pathology in ALS and PLS using tract-based spatial statistics. Hum. Brain Mapp. 30, 615–624. https://doi.org/10.1002/hbm.20527.

Clarke, J.L., Jackson, J.H., 1867. On a Case of Muscular Atrophy, with Disease of the Spinal Cord and Medulla Oblongata. Medico-Chir. Trans. 50 (489–498), 1. https://doi.org/10.1177/095952876705000122.

del Aguila, M.A., Longstreth, W.T., McGuire, V., Koepsell, T.D., van Belle, G., 2003. Prognosis in amyotrophic lateral sclerosis: a population-based study. Neurology 60, 813–819. https://doi.org/10.1212/01.wnl.0000049472.47709.3b.

Desikan, R.S., Ségonne, F., Fischl, B., Quinn, B.T., Dickerson, B.C., Blacker, D., Buckner, R.L., Dale, A.M., Maguire, R.P., Hyman, B.T., Albert, M.S., Killiany, R.J., 2006. An automated labeling system for subdividing the human cerebral cortex on MRI scans into gyral based regions of interest. NeuroImage 31, 968–980. https://doi.org/10.1016/j.neuroimage.2006.01.021.

Distaso, E., Milella, G., Mezzapesa, D.M., Introna, A., D'Errico, E., Fraddosio, A., Zoccolella, S., Dicuonzo, F., Simone, I.L., 2021. Magnetic resonance metrics to evaluate the effect of therapy in amyotrophic lateral sclerosis: the experience with edaravone. J. Neurol. 268, 3307–3315. https://doi.org/10.1007/s00415-021-10495-9.

Dubey, A.K., Gupta, U., Jain, S., 2016. Analysis of k-means clustering approach on the breast cancer Wisconsin dataset. Int. J. Comput. Assist. Radiol. Surg. 11, 2033–2047. https://doi.org/10.1007/s11548-016-1437-9.

Fischl, B., 2012. FreeSurfer. FreeSurfer. NeuroImage 62 (2), 774–781.

Floeter, M.K., Danielian, L.E., Braun, L.E., Wu, T., 2018. Longitudinal diffusion imaging across the C9orf72 clinical spectrum. J. Neurol. Neurosurg. Psychiatry 89, 53–60. https://doi.org/10.1136/jnnp-2017-316799.

Floeter, M.K., Katipally, R., Kim, M.P., Schanz, O., Stephen, M., Danielian, L., Wu, T., Huey, E.D., Meoded, A., 2014. Impaired corticopontocerebellar tracts underlie pseudobulbar affect in motor neuron disorders. Neurology 83, 620–627. https://doi.org/10.1212/WNL.0000000000000693.

Grachev, I.D., Berdichevsky, D., Rauch, S.L., Heckers, S., Kennedy, D.N., Caviness, V.S., Alpert, N.M., 1999. A method for assessing the accuracy of intersubject registration of the human brain using anatomic landmarks. NeuroImage 9, 250–268. https://doi.org/10.1006/nimg.1998.0397.

Grolez, G., Kyheng, M., Lopes, R., Moreau, C., Timmerman, K., Auger, F., Kuchcinski, G., Duhamel, A., Jissendi-Tchofo, P., Besson, P., Laloux, C., Petrault, M., Devedjian, J.C., Pérez, T., Pradat, P.F., Defebvre, L., Bordet, R., Danel-Brunaud, V., Devos, D., 2018. MRI of the cervical spinal cord predicts respiratory dysfunction in ALS. Sci. Rep. 8, 1828. https://doi.org/10.1038/s41598-018-19938-2.

Grolez, G., Moreau, C., Danel-Brunaud, V., Delmaire, C., Lopes, R., Pradat, P.F., El Mendili, M.M., Defebvre, L., Devos, D., 2016. The value of magnetic resonance imaging as a biomarker for amyotrophic lateral sclerosis: a systematic review. BMC Neurol. 16, 155. https://doi.org/10.1186/s12883-016-0672-6.

Grosskreutz, J., Kaufmann, J., Frädrich, J., Dengler, R., Heinze, H.-J., Peschel, T., 2006. Widespread sensorimotor and frontal cortical atrophy in Amyotrophic Lateral Sclerosis. BMC Neurol. 6, 17. https://doi.org/10.1186/1471-2377-6-17.

Hardiman, O., van den Berg, L.H., Kiernan, M.C., 2011. Clinical diagnosis and management of amyotrophic lateral sclerosis. Nat. Rev. Neurol. 7, 639–649. https://doi.org/10.1038/nrneurol.2011.153.

Iglesias, J.E., Van Leemput, K., Bhatt, P., Casillas, C., Dutt, S., Schuff, N., Truran-Sacrey, D., Boxer, A., Fischl, B., Alzheimer's Disease Neuroimaging Initiative,, 2015. Bayesian segmentation of brainstem structures in MRI. NeuroImage 113, 184–195. https://doi.org/10.1016/j.neuroimage.2015.02.065.

Jenkinson, M., Smith, S., 2001. A global optimisation method for robust affine registration of brain images. Med. Image Anal. 5, 143–156. https://doi.org/10.1016/s1361-8415(01)00036-6.

Lancaster, J.L., Woldorff, M.G., Parsons, L.M., Liotti, M., Freitas, C.S., Rainey, L., Kochunov, P.V., Nickerson, D., Mikiten, S.A., Fox, P.T., 2000. Automated Talairach atlas labels for functional brain mapping. Hum. Brain Mapp. 10, 120–131. https://doi.org/10.1002/1097-0193(200007)10:3<120::aid-hbm30>3.0.co;2-8.

H. Li, Q. Zhang, Q. Duan, J. Jin, F. Hu, J. Dang, M. Zhang, 2021, Brainstem involvement in amyotrophic lateral sclerosis: a combined structural and diffusion tensor MRI analysis. Front. Neurosci. 15, 675444. https://doi.org/10.3389/fnins.2021.675444.

Mezzapesa, D.M., D'Errico, E., Tortelli, R., Distaso, E., Cortese, R., Tursi, M., Federico, F., Zoccolella, S., Logroscino, G., Dicuonzo, F., Simone, I.L., 2013. Cortical thinning and clinical heterogeneity in amyotrophic lateral sclerosis. PloS One 8, e80748. https://doi.org/10.1371/journal.pone.0080748.

Miller, R.G., Jackson, C.E., Kasarskis, E.J., England, J.D., Forshew, D., Johnston, W., Kalra, S., Katz, J.S., Mitsumoto, H., Rosenfeld, J., Shoesmith, C., Strong, M.J., Woolley, S.C., 2009. Practice parameter update: the care of the patient with amyotrophic lateral sclerosis: drug, nutritional, and respiratory therapies (an evidence-based review): report of the Quality Standards Subcommittee of the American Academy of Neurology. Neurology 73 (15), 1218–1226.

Moore, S.R., Gresham, L.S., Bromberg, M.B., Kasarkis, E.J., Smith, R.A., 1997. A self report measure of affective lability. J. Neurol. Neurosurg. Psychiatry 63, 89–93. https://doi.org/10.1136/jnnp.63.1.89.

Pintzka, C.W.S., Hansen, T.I., Evensmoen, H.R., Håberg, A.K., 2015. Marked effects of intracranial volume correction methods on sex differences in neuroanatomical structures: a HUNT MRI study. Front. Neurosci. 9 https://doi.org/10.3389/fnins.2015.00238.

Poletti, B., Solca, F., Carelli, L., Faini, A., Madotto, F., Lafronza, A., Monti, A., Zago, S., Ciammola, A., Ratti, A., Ticozzi, N., Abrahams, S., Silani, V., 2018. Cognitive-behavioral longitudinal assessment in ALS: the Italian Edinburgh Cognitive and Behavioral ALS screen (ECAS). Amyotroph. Lateral Scler. Front. Degener. 19, 387–395. https://doi.org/10.1080/21678421.2018.1473443.

Ravits, J., Paul, P., Jorg, C., 2007. Focality of upper and lower motor neuron degeneration at the clinical onset of ALS. Neurology 68, 1571–1575. https://doi.org/10.1212/01.wnl.0000260965.20021.47.

Ravits, J.M., La Spada, A.R., 2009. ALS motor phenotype heterogeneity, focality, and spread: deconstructing motor neuron degeneration. Neurology 73, 805–811. https://doi.org/10.1212/WNL.0b013e3181b6bbbd.

Schuster, C., Elamin, M., Hardiman, O., Bede, P., 2016. The segmental diffusivity profile of amyotrophic lateral sclerosis associated white matter degeneration. Eur. J. Neurol. 23, 1361–1371. https://doi.org/10.1111/ene.13038.

Schuster, C., Hardiman, O., Bede, P., 2017. Survival prediction in Amyotrophic lateral sclerosis based on MRI measures and clinical characteristics. BMC Neurol. 17, 73. https://doi.org/10.1186/s12883-017-0854-x.

Schuster, C., Kasper, E., Machts, J., Bittner, D., Kaufmann, J., Benecke, R., Teipel, S., Vielhaber, S., Prudlo, J., 2014. Longitudinal course of cortical thickness decline in amyotrophic lateral sclerosis. J. Neurol. 261, 1871–1880. https://doi.org/10.1007/s00415-014-7426-4.

Spinelli, E.G., Riva, N., Rancoita, P.M.V., Schito, P., Doretti, A., Poletti, B., Di Serio, C., Silani, V., Filippi, M., Agosta, F., 2020. Structural MRI outcomes and predictors of disease progression in amyotrophic lateral sclerosis. NeuroImage Clin. 27, 102315 https://doi.org/10.1016/j.nicl.2020.102315.

Stambler, N., Charatan, M., Cedarbaum, J.M., 1998. Prognostic indicators of survival in ALS. ALS CNTF Treatment Study Group. Neurology 50 (1), 66–72.

Strong, M.J., Abrahams, S., Goldstein, L.H., Woolley, S., Mclaughlin, P., Snowden, J., Mioshi, E., Roberts-South, A., Benatar, M., HortobáGyi, T., Rosenfeld, J., Silani, V., Ince, P.G., Turner, M.R., 2017. Amyotrophic lateral sclerosis - frontotemporal spectrum disorder (ALS-FTSD): Revised diagnostic criteria. Amyotroph. Lateral Scler. Front. Degener. 18, 153–174. https://doi.org/10.1080/21678421.2016.1267768.

Trojsi, F., Di Nardo, F., Siciliano, M., Caiazzo, G., Passaniti, C., D'Alvano, G., Ricciardi, D., Russo, A., Bisecco, A., Lavorgna, L., Bonavita, S., Cirillo, M., Esposito, F., Tedeschi, G., 2021. Resting state functional MRI brain signatures of fast disease progression in amyotrophic lateral sclerosis: a retrospective study. Amyotroph. Lateral Scler. Front. Degener. 22, 117–126. https://doi.org/10.1080/21678421.2020.1813306.

Tu, S., Huang, M., Caga, J., Mahoney, C.J., Kiernan, M.C., 2021. Brainstem Correlates of Pathological Laughter and Crying Frequency in ALS. Front. Neurol. 12, 704059 https://doi.org/10.3389/fneur.2021.704059.

Voevodskaya, O., Simmons, A., Nordenskjöld, R., Kullberg, J., Ahlström, H., Lind, L., Wahlund, L.-O., Larsson, E.-M., Westman, E., Alzheimer's Disease Neuroimaging Initiative,, 2014. The effects of intracranial volume adjustment approaches on multiple regional MRI volumes in healthy aging and Alzheimer's disease. Front. Aging Neurosci. 6, 264. https://doi.org/10.3389/fnagi.2014.00264.

Wainger, B.J., Macklin, E.A., Vucic, S., McIlduff, C.E., Paganoni, S., Maragakis, N.J., Bedlack, R., Goyal, N.A., Rutkove, S.B., Lange, D.J., Rivner, M.H., Goutman, S.A., Ladha, S.S., Mauricio, E.A., Baloh, R.H., Simmons, Z., Pothier, L., Kassis, S.B., La, T., Hall, M., Evora, A., Klements, D., Hurtado, A., Pereira, J.D., Koh, J., Celnik, P.A., Chaudhry, V., Gable, K., Juel, V.C., Phielipp, N., Marei, A., Rosenquist, P., Meehan, S., Oskarsson, B., Lewis, R.A., Kaur, D., Kiskinis, E., Woolf, C.J., Eggan, K., Weiss, M.D., Berry, J.D., David, W.S., Davila-Perez, P., Camprodon, J.A., Pascual-Leone, A., Kiernan, M.C., Shefner, J.M., Atassi, N., Cudkowicz, M.E., 2021. Effect of Ezogabine on Cortical and Spinal Motor Neuron Excitability in Amyotrophic Lateral Sclerosis: A Randomized Clinical Trial. JAMA Neurol. 78, 186–196. https://doi.org/10.1001/jamaneurol.2020.4300.

Winkler, A.M., Ridgway, G.R., Webster, M.A., Smith, S.M., Nichols, T.E., 2014. Permutation inference for the general linear model. NeuroImage 92, 381–397. https://doi.org/10.1016/j.neuroimage.2014.01.060.

Zhang, Y., Brady, M., Smith, S., 2001. Segmentation of brain MR images through a hidden Markov random field model and the expectation-maximization algorithm. IEEE Trans. Med. Imaging 20, 45–57. https://doi.org/10.1109/42.906424.